Industrial Engineering Journal
ISSN: 0970-2555
Volume : 53, Issue 7, July : 2024

A Common DC-Bus-Configured Traction Motor Emulator Using a Virtually Isolated Three-Phase AC-DC Bidirectional Converter

S.GURU BHASKAR REDDY PG Student, Dept of EEE, SITS, Kadapa.
SHAIK WAZEED Assistant Professor, Dept of EEE, SITS, Kadapa.

Abstract –

The current state-of-the-art development process for electric system applications is based on segregated simulation and testing activities. An industrial drive testing, with a `real-machine' can pave way, for some serious issues to test-bench and motor. A slight disturbance in control logic amid testing, can damage the physical machine or drive. Such dangerous testing conditions can be avoided by supplanting real motor with a power electronic converter based `Motor Emulator' (ME) test-bench system. The conventional ME comprises of two-stage three-phase AC-DC-AC conversion with first-stage AC-DC as emulator and second-stage DC-AC as regenerating unit. This two-stage power conversion, require independent control algorithm, burdening control complexity as well as the number of power electronic switches are quite significant. Hence, to economize and downsize conventional multistage ME system, this project experimentally validates a common DC-bus-configured ME system with only the AC-DC regenerative emulator stage. A virtually isolated bidirectional two-level three-phase AC-DC converter is proposed as the regenerative emulator converter in a common DC-Bus-configured ME system. The Proposed converter's operating principle along with mathematical design and control strategy are also presented. To validate the operation of the proposed converter as a common DC-bus-configured emulator, permanent magnet synchronous motors (PMSM) is emulated and its Simulation results are presented with a Proportional + Integral (PI) and also Artificial neural network (ANN) control structure was chosen and implemented. This project presents several enhancements to maximise the performance of this controller.

Keywords – AC-DC, bidirectional converter, buck-boost, DC-AC, device under test, motor emulator, permanent magnet synchronous motor, synchronous converter.

I. INTRODUCTION

In power systems, and especially distribution systems, power electronic devices are getting more common. They are utilized both as interfaces in customer loads, and as a solution in the grid itself. One reason behind the later, is the increased interest in power quality, a term which targets the quality of the voltages and currents, focused on distortions from ideal power supplies. With respect to power quality, power electronic based loads are, on one hand, more demanding than conventional loads. At the same time, these loads tend to pollute the power system with more power quality related issues. One solution, for improving the power quality, is to use power electronic controllers. The conventional test-rig setup with the real electric machine for testing the motor drives has some drawbacks, such as extended test time, huge space requirement, high energy consumption, higher operation and maintenance cost as well as large equipment complexity. The need of replacing physical electric motor for testing drive at various load configurations, further adds on operating cost and complexity of the system. Integration of power electronics together with software simulation is being used for developing a hardware-in-loop (HIL) system for emulating an electric motor. This power electronic system capable of emulating motor characteristics is known as `motor emulator' (ME). In traditional ME, real rotating machine is replaced with AC-DC-AC multistage, power electronic converter. The motor model estimates the phase, frequency and magnitude of current for a specific motor for the applied voltage input at motor terminals by drive. Further, based on control strategy implemented, the emulating converter is controlled in such a way that, current drawn from `Device Under Test' or `Drive Under Test' (DUT) mimics the estimated reference current by motor model. The advantage of such ME system is, flexible load configuration. A ME system comprises of two back-to-back AC-DC and DC-AC power converters. Where former, operates as an emulator and later as a regenerating unit. The output of regeneration unit is interfaced with utility grid, to act as `sink' or `source' in case of motoring or regenerative braking operation respectively. This two-stage arrangement forming AC-AC PWM (pulse width modulation) Cyclo converter with common DC link capacitor, requires independent control and increases controller complexity. The dc-link element ensures the decoupling between two converter stages. This entrench that, a constant source is available at the input of DC-AC inverter stage, which increases the converter's power capability. However, the dc-link element can have a relatively large size compared with the total converter size.

To simplify the control algorithm and to reduce the number of converter stages, a common DC-bus ME system architecture where output of the AC-DC converter stage is fed back to DC source of the DUT. The structure of ME with common DC bus, where DUT input as well as DC side of the proposed converter is supplied with a common DC source. Unlike the conventional system, where three-phase AC output of the regenerator converter is fed back to the utility, the output power of proposed converter is fed back to the common DC source. Although, motor emulators are existing for over two decades, there has been little to no research focus on simplifying the whole system by optimizing power converter topology used as an emulator. The converter topology used makes use of 17-level Double Star Chopper Cell (DSCC). The multilevel converters have their own advantages, however, the number of power semiconductor switches increase as the level increases resulting in increased switching losses. Therefore, as an attempt to simplify the whole ME architecture, including converter topology, this project proposes a virtually isolated bidirectional three-phase AC-DC converter based on synchronous buck-boost operation. This project follows the extended version with slightly upgraded converter topology in terms of LCL filter replacing LC filter.

II. STATE-OF-THE-ART BATTERY CHARGING POWER CONVERTERS

Galvanic isolation is preferred or required to meet the safety requirement of the standards for EV charging when connecting to the utility grid. Reinforced or double insulation is required to meet IEEE EV fast charger standard. The EV body must be connected to earth during charging. When the charger has no internal electrical separation, isolation monitoring is essential, and the battery must be isolated from the car body. Galvanic isolation within the converter will eliminate the need for a separate isolation transformer on the utility side. Good efficiency over a wide output voltage is a required feature for battery chargers. The open circuit voltage of a battery can change significantly from full state of charge to zero state of charge. Hence, the converter should be able to efficiently operate over wide voltage range. Higher efficiency at full load means lower thermal requirements. This will allow lower cost cooling options or lower volume for cooling. With larger battery packs in bus, trucks and other heavy vehicles the charging rate is usually limited by the charger power rating. Also, electric cars with battery packs with high charge rate are being introduced by car manufacturers. These applications demand very high power chargers. Power converter topologies capable for handling high power are required.

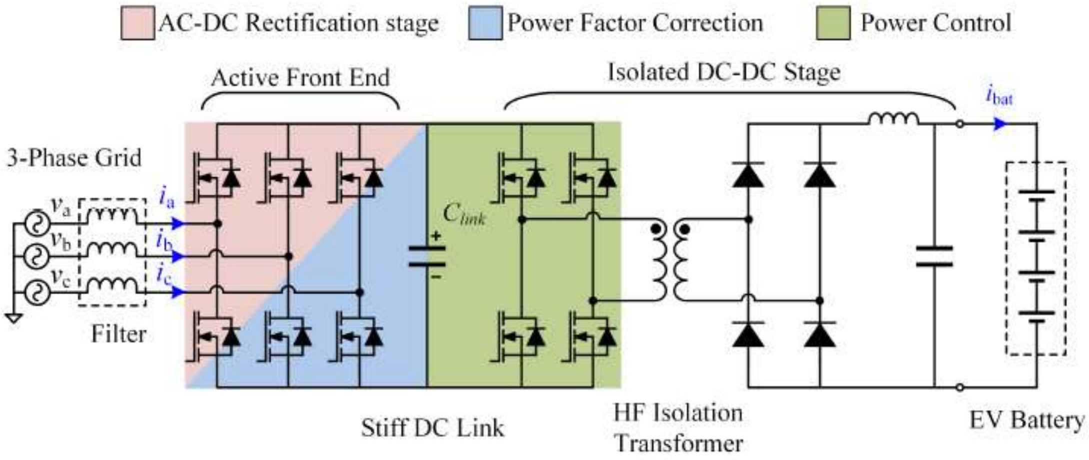

Fig. 1: State-of-the-art converter topology for high power battery charging

Battery charging applications also require a current and a voltage source characteristic of the power supply, which means it has to be able to control the output voltage and to limit the output current in case of a short circuit. State-of-the-art (SOA) solutions for high power battery charging systems are typically implemented as two-stage systems, comprising a Power Factor Correction (PFC) rectifier input stage followed by an isolated DC-DC converter. This approach allows the use of a simple and well-understood AC/DC Active Front End (AFE) rectifier and standard 2-level isolated H-bridge topologies in the DC-DC stage. Different topologies are possible for the AC-DC and DC-DC stages. A review of some of the possible converter topologies in given. A 2-level Voltage Source Converter (VSC) is commonly used as AFE. The VSC is Pulse Width Modulated (PWM) to shape the line currents sinusoidal and maintains a stiff intermediate DC link. An input LCL grid filter is typically employed to attenuate the harmonics to be compliant to the harmonic injection standards. The cascade DC-DC converter has a high-frequency transformer to provide galvanic isolation. For high power chargers three-level AC-DC rectifiers are gaining popularity. Due to the three-level switching, the voltage stress on the devices is lower; switching loss per device is reduced allowing a higher frequency switching. The 3-level switching node also reduces the required attenuation for grid filter. LLC resonant converter and phase-shifted full-bridge converter are two of the most popular topologies used in this stage. In the topology shown in Fig. 1, a phase shift full-bridge (PSFB) topology is used for the dc-dc stage. PSFB is extensively used for various DC-DC applications and well-studied in literature. Dedicated control ICs are available to implement the control. This topology continues to get attention from researchers and new modulation techniques are being reported that improve the performance of this topology further. 50 kW PSFB designs are reported for DC fast charging application. A study between single-phase and three-phase is presented in this work. This topology has the advantage of an easy controllability with a single control parameter (i.e phase-shift between the H-bridge legs) and of a high efficiency due to ZVS where only a small circulating energy is required. The drawback of the PSFB converter is the over-voltage occurring at the secondary rectifier devices due to resonances between parasitic elements. A snubber or a clamp circuit is necessary, as discussed later in this chapter. Multiple effective methods have reported to address the parasitic resonance. PSFB is uniquely suitable for battery charging system requirements. Usually, the system specification requires a current source and a voltage source characteristic of the power supply, which means it has to be able to control the output voltage and to limit the output current in case of a short circuit. This requirement can be easily fulfilled by the PSFB topology. To summarize about PSFB, the topology is simple, reliable, and proven to be effective for battery charging applications. In two-stage approach the dc-link voltage is actively controlled by the AC-DC stage. This allows changing the DC-link voltage to optimize the converter performance based on the operating point. This additional exibility provided can used to reduce the voltage gain variation for the DC-DC stage. With narrow voltage gain specification, resonant DC-DC topologies can be effective option. In particular, LLC resonant topology has been explored for battery charging application. Half bridge LLC topology has been very popular with consumer electronics power supply industry. Low profile planar transformers are required in power supplies for at TVs. Leakage inductance of these transformer tend to be higher. LLC is preferred topology since this topology effectively utilizes the leakage inductance of the transformer as a circuit element for power transfer. For higher power (>500 W) Fullbridge LLC is preferred because of better utilization of the transformer and reduction in current stress of the components. Compared to PSFB the output filter capacitor can be larger. Higher capacitance value is required to meet the ripple criteria and large number of capacitors are usually required to meet the ripple current rating. The wide choice of design parameters available in LLC topology make the optimal design of LLC difficult. Full order analysis is involving, fundamental harmonic approximation is typically used which has lower accuracy. Nonetheless, researchers have been exploring to use LLC for battery charging application. Using variable DC-link voltage the voltage range required for LLC is reduced. To reduce the output filter capacitance interleaving of converter modules can be used. There is on-going research on advanced modulation techniques for efficient operation over a wider voltage range. The two-stage approach gives tight, highly dynamic control of the output voltage levels to disturbances on grid side voltages. Simple control techniques are adequate due to the decoupling provided by the intermediate DC link. EV charging applications do not demand high dynamic performance from the converter. Since the reference commands to the charger in both constant current (C.C) and constant voltage (C.V.) output modes of charging are slow varying values, high dynamic performance is not required, and having a stiff DC link is not necessary. Stiff dc link is usually necessary when energy buffering is required, for example, to provide some hold-up time after grid failure. Since both the converter stages are switching at high frequency, switching loss occurs, and filters are required in the two stages. And usually, the AFE is a hard-switched topology that limits the operating frequency (below 20 kHz) and hence power density. Switching frequency in the range below 20 kHz cause audible noise, and hence noise attenuation measurements are required. The state-of-the-art commercial 50 kW chargers have an efficiency of around 94% at nominal load. Compared to the SOA stiff DC-link, soft DC-link based two-stage rectifier topologies improve the achievable efficiency and power density. The improvements are achieved by reducing the duration for which the front-end rectifier is switched at high frequency. For example, the devices in the VSC operate at HF for just 1/3rd of the time. Three-phase unfolding based rectification is one such method that completely avoids high frequency switching in the front-end AC-DC stage. This eliminates the switching loss in the front-end rectification stage and also minimizes the filtering requirement on the utility side. System efficiency and power density can be improved by using three phase unfolding rectification. The unfolding based converters can meet all the application requirements while greatly improving efficiency and power density. The idea is similar to the popular 1-phase unfolding approach typically used for solar inverters but adapted for 3-ph 3 wire systems.

III. PROPOSED SYSTEM

The primary goal of traction motor emulator is to design and develop a power electronics converter based controlled load as an replacement for the actual traction machine load. Subsequently, the behavior of the traction machine emulator should be as close as the electrical characteristics of the real traction machine load when driven by a DUT. The traditional traction motor emulator configuration is as demonstrated in Fig. 2, where the emulator converter is driven by the three-phase DUT output voltage. Thus, detailed information of the phase, frequency and magnitude of the DUT output voltages is of prime importance. The core element of traction motor emulator is the mathematical model of electric motor under emulation, that estimates the phase frequency and magnitude of the desired currents to be drawn so as to imitate the real electric machine. Further, the control algorithm ensures that three-phase currents drawn or supplied by the ME are matching with that of the estimated current references. The ME is driven by the DUT and both the power electronics converters coupled to each other through L or LCL filter. Since the ME imitates the electrical characteristics of an real electric traction motor, it would have to either absorb or supply power as per the quadrant of operation of the electric motor under emulation. To empower the ME to be a `sink' or `source' of power, two back-to-back VSI (voltage source inverter) forming a two-level AC-AC cyclo-converter is used.

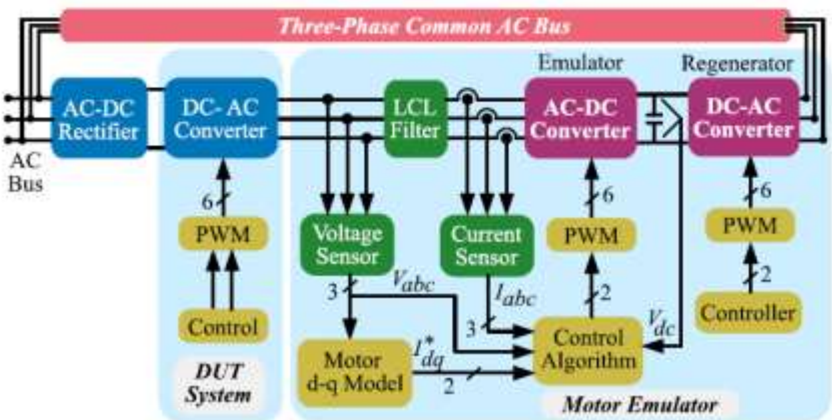

Fig:2 Block diagram of classical motor emulator.

The dc link element is common to both emulator and re-generator VSI. The three-phase voltage output of re-generator VSI converter is fed to the AC utility grid. This re-generator VSI absorbs or supplies power from the utility grid for the emulator VSI. A ME system comprises of two back-to-back AC-DC and DC-AC power converters as shown in Fig. 2. Where former, operates as an emulator and later as a regenerating unit. The output of

Industrial Engineering Journal
ISSN: 0970-2555
Volume : 53, Issue 7, July : 2024

regeneration unit is interfaced with utility grid, to act as `sink' or `source' in case of motoring or regenerative braking operation respectively. This two-stage arrangement forming AC-AC PWM (pulse width modulation) Cyclo converter with common DC link capacitor, requires independent control and increases controller complexity.

The dc-link element ensures the decoupling between two converter stages. This entrench that, a constant source is available at the input of DC-AC inverter stage, which increases the converter's power capability. However, the dc-link element can have a relatively large size compared with the total converter size. To simplify the control algorithm and to reduce the number of converter stages, a common DC-bus ME system architecture was presented where output of the AC-DC converter stage is fed back to DC source of the DUT. The structure of ME with common DC bus is shown in Fig. 3, where DUT input as well as DC side of the proposed converter are supplied with a common DC source. Unlike the system shown in Fig. 2, where three-phase AC output of the regenerator converter is fed back to the utility, the output power of proposed converter is fed back to the common DC source. Although, motor emulator are existing for over two decades, there has been little to no research focus on simplifying the whole system by optimizing power converter topology used as an emulator.

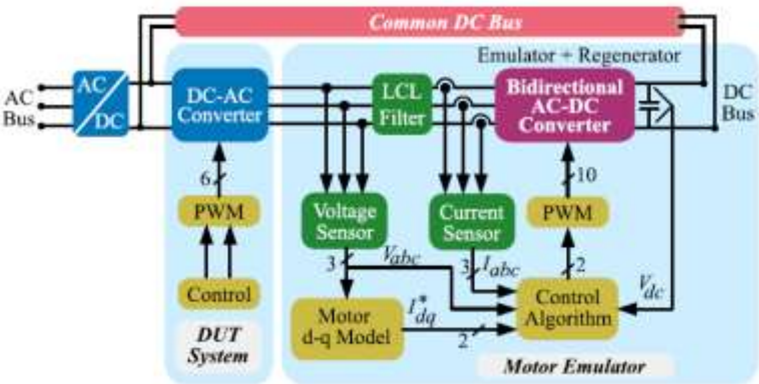

Fig:3 Block diagram of common DC-bus-configured motor emulator.

The converter topology used makes use of 17-level Double Star Chopper Cell (DSCC). The multilevel converter have their own advantages, however, the number of power semiconductor switches increase as the level increases resulting in increased switching losses. Therefore, as an attempt to simplify the whole ME architecture, including converter topology, this project proposes a virtually isolated bidirectional three-phase AC-DC converter based on synchronous buck-boost operation. This project follows the extended version of previous project by authors with slightly upgraded converter topology in terms of LCL filter replacing LC filter.

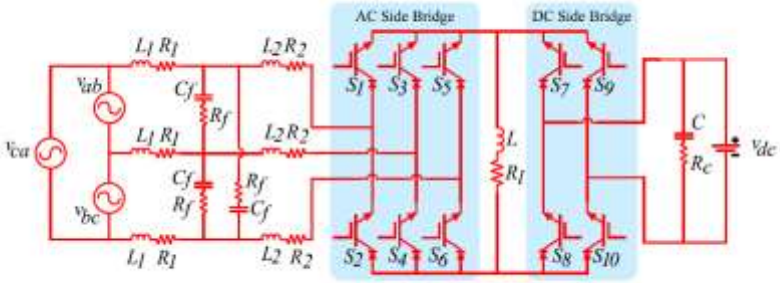

Fig:4 Proposed bi-directional buck-boost 3-Φ AC-DC converter.

Numerous researchers have proposed 3-Φ AC-DC converter topologies with buck, boost, buck-boost mode of operation. A detailed review of three-phase AC-DC converter is presented. A 3-Φ step-down bi-directional AC-DC converter topology was proposed. A similar approach can be considered for 3-Φ bi-directional AC-DC buck-boost converter. However, this would require twelve power semiconductor switches. A single-switch three-phase AC-DC converter topology was proposed in and an upgraded topology was proposed. Another single switch buck-boost three-phase AC-DC converter topology was proposed. The three-phase diode bridge-rectifier, used in these topologies would block reverse power flow in braking mode. Thus, AC-DC converter with diode bridge rectifier, makes them unsuitable for the ME system. A three-phase single-stage AC-DC PWM full bridge converter was proposed. Although single-stage AC-DC conversion is possible, only the buck operation provided by this topology is not desired for ME application. Another interesting converter topology providing low current THD (Total Harmonic Distortion) was proposed consisting of buck-boost inductor in each leg of converter bridge. An isolated bi-directional AC-DC converter topology comprising of eighteen power semiconductor switches was proposed. However, isolated converter topology is unsuitable for ME, as for low speed emulation, the isolation transformer coil magnetization is insufficient to generate secondary voltage, resulting in poor emulation performance. These factors associated with aforementioned converter topologies, highly demand a reduced switch, bi-directional, non-isolated AC-DC converter topology. In addition, single-stage reverse power control is also desired. Hence, for common DC bus ME application, with little modification in the 3-Φ AC-DC converter topology presented a bi-directional buck-boost AC-DC converter topology was presented. The proposed converter topology has been improved from the one presented. The LC filter in the converter topology presented has been replaced with LCL filter to reduce the stress on converter switches. Furthermore, the operating principle has also been modified to achieve desired buck-boost operation. The proposed converter topology is presented in Fig. 4. For simple understanding of proposed converter operation, detailed schematic of common DC bus ME system along with proposed converter, control strategy and PMSM model are not shown here. The proposed converter in Fig. 4 replaces `Bidirectional AC-DC Converter' block in Fig. 3. Referring to Fig. 4, three-phase unfiltered voltages, vab, vbc and vca from DUT are applied as input to the proposed converter. On the output side, there is common DC bus, vdc, which connects both ME output and DUT input. It is to be noted that, throughout this project, vdc represents common DC bus voltage. The output voltage of proposed converter is measured across DC Link capacitor C. Inductor L is buck-boost inductor, capacitor C is DC link capacitor. The operation of proposed converter topology is further explained for forward motoring and forward braking mode of operation of AC machine. The operation of during reverse motoring and reverse braking is same as that of forward motoring and forward braking except the fact that, two of the three-phases are swapped. The operation of proposed converter is discussed based on SVPWM (space vector pulse width modulation) technique. It is well known phenomenon that, a SVPWM cycle comprises of two active vectors and one zero (null) vector. This phenomenon is used to achieve virtual isolation between the three-phase AC and DC sides of the proposed converter. During the active states, DC side full bridge of the proposed converter is virtually isolated as it is kept OFF for the entire active state duration. Whereas, during zero state, the energy stored in buck-boost inductor is dissipated into common DC bus through DC side full bridge. While in zero state, either all upper or lower switches from AC side three-phase bridge are ON, resulting in virtual isolation from DC side full bridge. Here, the duration of active vectors are denoted as T1 and T2, whereas that of zero vector is denoted as T0. The AC side converter switches S1 to S6 forms a two-level PWM converter converting 3-Φ input AC voltage from DUT to DC which appears across the buck-boost inductor L. At any instant the voltage appearing across inductor L is (Γ3.vi), where vi is input phase voltage.

IV. SIMULATION RESULTS

Industrial Engineering Journal
ISSN: 0970-2555
Volume : 53, Issue 7, July : 2024

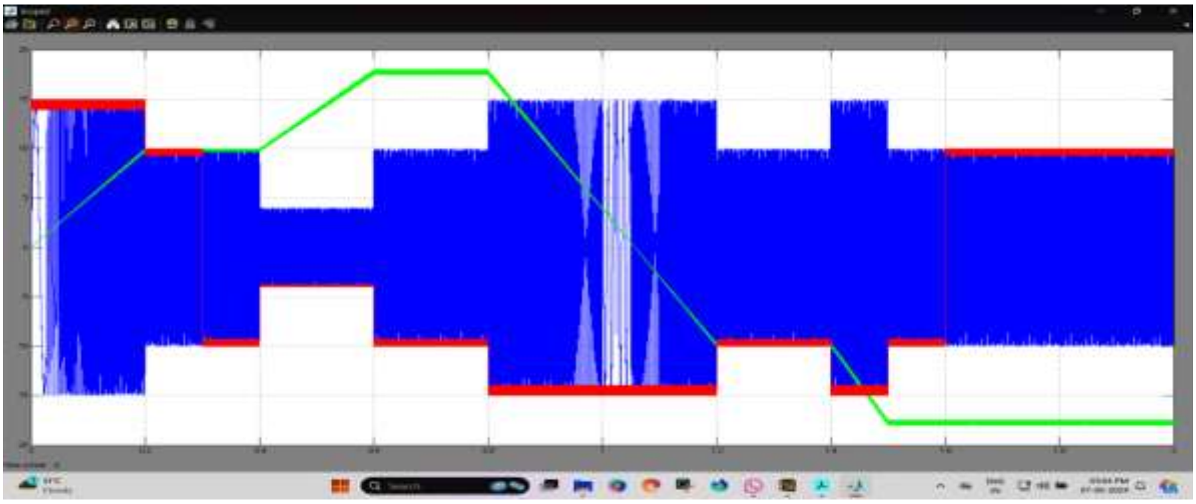

Fig:5 simulation waveform of PMSM motor. (Existing System)

The simulation waveforms represents rotor speed and electromagnetic torque estimated by motor model respectively.

Fig:6 zoomed waveforms from 0s to 0.5s.

As shown in Fig. 6, at time *t* = 0 *s*, both speed and torque commands are set to 500 *RPM* and 10 *Nm* respectively. With these test commands, the emulator is expected to emulate first quadrant (forward motoring) of operation of PMSM motor under study. Until 0.2 *s*, when motor attains desired 500 *RPM* speed, the emulator draws high current to emulate high starting torque as can be seen in Fig. 6. As soon as the emulated speed reaches to desired speed reference, emulator starts drawing nominal current and electromagnetic torque drops down to its reference value i.e. 10 *Nm*. The torque remains constant to 10 *Nm* until the next test command, which appears at 0.3 *s*. For initial three seconds, the ME system emulates forward motoring operation. At 0.3 *s*, the torque command changes to -10 *Nm* to force emulation of forward braking operation. It is visible in Fig. 6 that, as soon as the torque

Industrial Engineering Journal
ISSN: 0970-2555
Volume : 53, Issue 7, July : 2024

command changes the, the emulated torque drops to -10 *Nm* and phase-A current reverses. A minor spike in current as well as speed waveform can be noticed in Fig. 6. However, emulator still draws, the 10 *A* peak current from DUT. At 0.4 *s*, the speed reference is changed to 900 *RPM* and to operate in constant torque region, the electromagnetic torque increases from -10 *Nm* to -4 *Nm*.

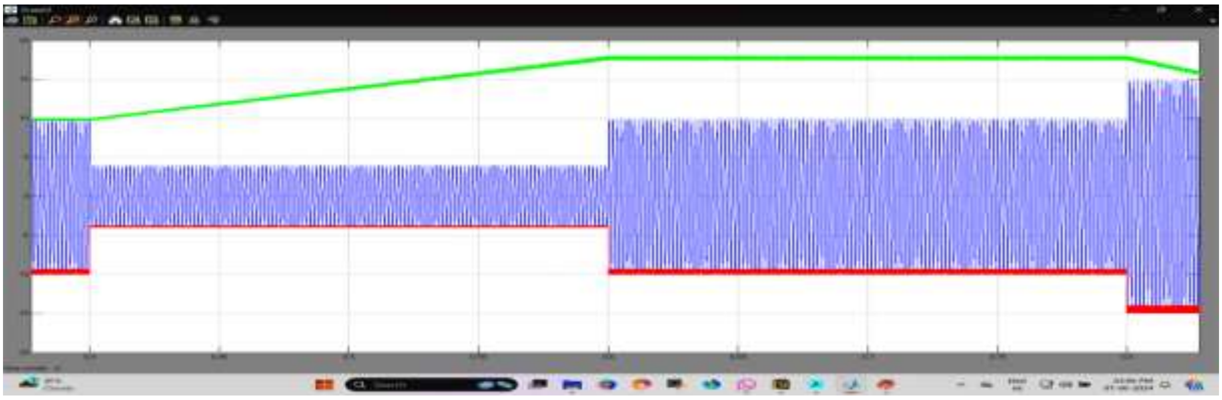

Fig:7 zoomed waveforms from 0.4s to 0.8s

At 0.6 *s*, the emulator speed attains the desired reference of 900 *RPM* as shown in Fig. 7. The electromagnetic torque returns to the -10 *Nm* reference mark and remains steady until next test command appears at 0.8 *s*. As the speed reference is dropped to -500 *RPM* at 0.8 *s*, the braking current increases to approximately 15 *A* peak. The emulator, draws high braking current until rotor speed is dropped to zero at approx. 1.025 *s*. At this instance, the forward braking operation ends.

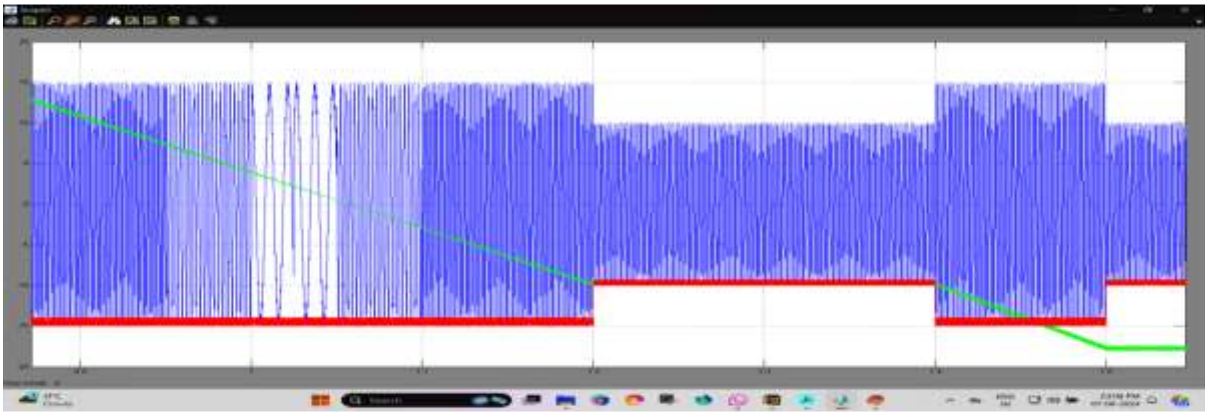

Fig:8 zoomed waveforms from 0.8s to 1.6s

Industrial Engineering Journal
ISSN: 0970-2555
Volume : 53, Issue 7, July : 2024

At 1.025*s*, speed as well as phase reversal occurs as shown in Fig. 8. The emulated rotor speed further drops linearly in negative direction (reverse motoring) until desired speed is attained at 1.2*s*. The electromagnetic torque returns to its reference value of -10 *Nm* and remains constant until next test command appears at 1.4*s*. At 1.4 *S*, the reference speed is further increased in reverse direction to -900 *RPM*, as shown in Fig. 8. The DUT supplies, the high current demand during speed increment until speed is reached to -900 *RPM* at 1.5 *s*. The reverse motoring operation continues till 1.6 *s* when next test command appears.

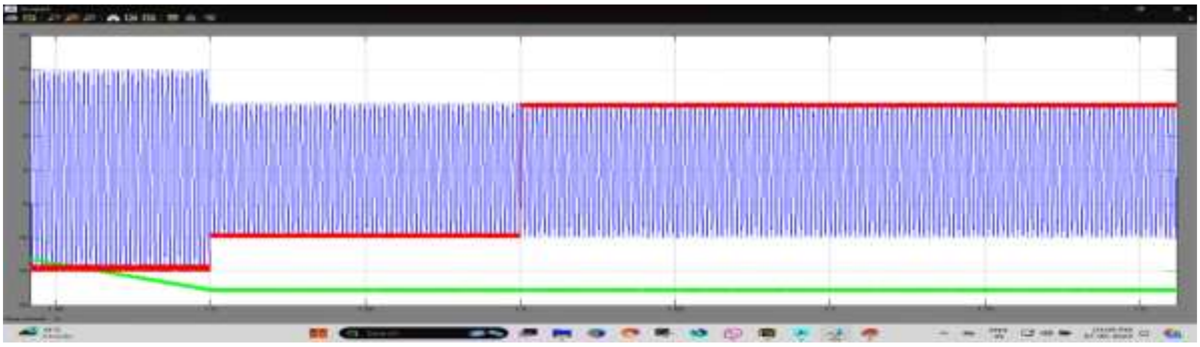

Fig:9 zoomed waveforms from 1.4s to 2s

As shown in Fig. 9, at 1.6 *s*, the torque reference is changed from -10 *Nm* to 10 *Nm*, to force reverse braking operation. This sudden braking causes minor spike in current signal, as can be noticed in Fig. 9.

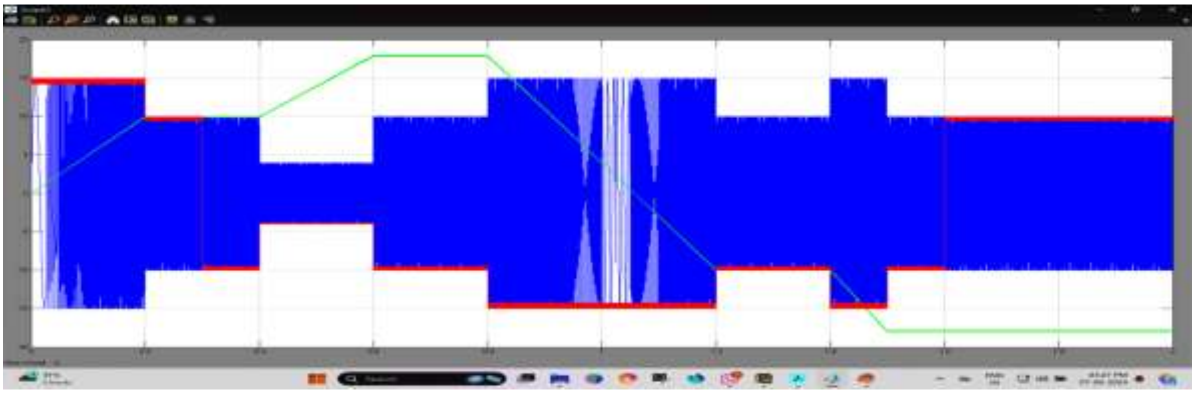

Fig:10 simulation waveform of PMSM motor. (Proposed System)

V. CONCLUSION

A simplified virtually isolated, bidirectional, three-phase AC-DC converter for ME system is proposed in this project. The proposed bi-directional converter inspired from classical buck-boost operation, requires just ten unidirectional IGBT switches. The unidirectional IGBT swtiches prevents any circulating current in the system. The proposed converter also takes out the regenerative converter stage in classical ME system. Also, the proposed common DC-bus-configured ME system requires a single stage control unlike independent control in existing ME system. The proposed converter provides four-quadrant operation and emulation of motor under study. The proposed ME converter can be made to draw the same current as a real machine would have drawn, had it been driven by the same DUT. The PMSM motor model is used to estimate the reference current used for controlling the proposed converter. This provides re-configuration ability to ME system. Since, the DC output current of proposed converter is fed back to DC bus, the overall input power source requirement is reduced. Overall, by analyzing experimental results, it is verified that, proposed virtually isolated, bidirectional AC-DC converter topology is a feasible alternative for conventional ME system with AC-DC-AC converter, providing simple common control.

REFERENCES

[1] R. S. Kaarthik, K. S. Amitkumar, and P. Pillay, ``Emulation of a permanent magnet synchronous generator in real-time using power hardware-in-the loop," IEEE Trans. Transport. Electric., vol. 4, no. 2, pp. 474_482, Jun. 2018.

[2] K. S. Amitkumar, R. S. Kaarthik, and P. Pillay, ``A versatile power hardware- in-the-loop-based emulator for rapid testing of transportation electric drives," IEEE Trans. Transport. Electric., vol. 4, no. 4, pp. 901_911, Dec. 2018.

[3] M. Oettmeier, R. Bartelt, C. Heising, V. Staudt, A. Steimel, S. Tietmeyer, B. Bock, and C. Doerlemann, ``Machine emulator: Power-electronics based test equipment for testing high-power drive converters," in Proc. 12th Int. Conf. Optim. Electr. Electron. Equip., May 2010, pp. 582_588.

[4] Y. S. Rao and M. C. Chandorkar, ``Real-time electrical load emulator using optimal feedback control technique," IEEE Trans. Ind. Electron., vol. 57, no. 4, pp. 1217_1225, Apr. 2010.

[5] O. Vodyakho, M. Steurer, C. S. Edrington, and F. Fleming, ``An induction machine emulator for high-power applications utilizing advanced simulation tools with graphical user interfaces," IEEE Trans. Energy Convers., vol. 27, no. 1, pp. 160_172, Mar. 2012.

[6] D. J. Atkinson, A. G. Jack, and H. J. Slater, ``The virtual machine [power electronic conversion equipment testing]," in Proc. IEE Colloq. Vector Control, Feb. 1998, pp. 7-1_7-6.

[7] J.W. Kolar, T. Friedli, J. Rodriguez, and P.W. Wheeler, ``Review of three phase PWM AC_AC converter topologies," IEEE Trans. Ind. Electron., vol. 58, no. 11, pp. 4988_5006, Nov. 2011.

[8] A. H. Kadam, R. Menon, and S. S. Williamson, ``A novel bidirectional three-phase AC_DC/DC-AC converter for PMSM virtual machine system with common DC bus," in Proc. IEEE Appl. Power Electron. Conf. Expo. (APEC), San Antonio, TX, USA, Mar. 2018, pp. 1944_1951.

[9] K. Saito and H. Akagi, ``A real-time real-power emulator of a medium voltage high-speed induction motor loaded with a centrifugal compressor," IEEE Trans. Ind. Appl., vol. 55, no. 5, pp. 4821_4833, Sep. 2019.

[10] I. Abdelsalam, G. P. Adam, D. Holliday, and B. W. Williams, ``Single stage AC_DC buck-boost converter for medium-voltage high-power applications," IET Renew. Power Gener., vol. 10, no. 2, pp. 184_193, 2016.

[11] T. C. Green, M. H. Taha, N. A. Rahim, and B. W. Williams, ``Three phase step-down reversible AC_DC power converter," IEEE Trans. Power Electron., vol. 12, no. 2, pp. 319_324, Mar. 1997.

[12] E. H. Ismail and R. Erickson, ``Single-switch 3-_ PWM low harmonic rectifiers," IEEE Trans. Power Electron., vol. 11, no. 2, pp. 338_346, Mar. 1996.

[13] D. S. Wijeratne and G. Moschopoulos, ``A novel three-phase buck_boost AC_DC converter," IEEE Trans. Power Electron., vol. 29, no. 3, pp. 1331_1343, Mar. 2014.

[14] I. Abdelsalam, G. P. Adam, D. Holliday, and B.W.Williams, ``Three-phase AC_DC buck-boost converter with a reduced number of switches," IET Renew. Power Gener., vol. 9, no. 5, pp. 494_502, 2015.

[15] D. S. Wijeratne and G. Moschopoulos, ``A three-phase single-stage AC_ DC PWM buck-type full-bridge converter: Analysis, design, and characteristics," IEEE Trans. Ind. Electron., vol. 60, no. 10, pp. 4201_4214, Oct. 2013.

[16] L.-S. Yang, T.-J. Liang, and J.-F. Chen, ``Analysis and design of a novel three-phase AC_DC buck-boost converter," IEEE Trans. Power Electron., vol. 23, no. 2, pp. 707_714, Mar. 2008.

[17] L. Gu and K. Jin, ``A three-phase isolated bidirectional AC/DC converter and its modified SVPWM algorithm," IEEE Trans. Power Electron., vol. 30, no. 10, pp. 5458_5468, Oct. 2015.

[18] L. Gu and K. Jin, ``A three-phase bidirectional AC/DC converter with Y-M connected transformers," IEEE Trans. Power Electron., vol. 31, no. 12, pp. 8115_8125, Dec. 2016.

[19] V. F. Pires and J. F. A. Silva, ``Single-stage three-phase buck-boost type AC_DC converter with high power factor," IEEE Trans. Power Electron., vol. 16, no. 6, pp. 784_793, Nov. 2001.

[20] B. Singh, B. N. Singh, A. Chandra, K. Al-Haddad, A. Pandey, and D. P. Kothari, ``A review of three-phase improved power quality AC_DC converters," IEEE Trans. Ind. Electron., vol. 51, no. 3, pp. 641_660, Jun. 2004.